

Replica Theory of Granular Media

Jeferson J. Arenzon

Instituto de Física – UFRGS

CP 15051 – 91501-970 – Porto Alegre RS – BRAZIL

E-mail: arenzon@if.ufrgs.br

Homepage: www.if.ufrgs.br/~arenzon

(June 25, 1998)

An infinite range spin glass like model for granular systems is introduced and studied through the replica mean field formalism. Equilibrium, density dependent properties under vibration and gravity are obtained.

Handling of granular material is present in many agricultural and industrial processes and several fundamental practical problems are still unsolved. Besides that, their unusual static and flow properties [1] offer a challenging problem from the theoretical point of view, and despite the huge effort that has been devoted in recent years, are far from being fully understood. Since thermal energy plays no role here, excitations can be achieved by externally shaking or shearing the system, enabling them to wander through the many microscopic configurations available for a fixed macroscopic density. Under vibration, a multitude of fascinating phenomena show up, like heap formation, convection cells, size or shape segregation, surface waves, etc (see [1] for a review and references). Another effect is the logarithmically slow rate of the density increase as the system suffers a sequence of taps [2]. This slow relaxation phenomenon under perturbations, signalling complex cooperative movements of the particles, resembles the one found in systems with many metastable states like glasses and spin glasses.

The analogy between glassy and granular behavior has been suggested some time ago [1] and stressed recently along with the role of geometric frustration [3]. This frustration arises from the excluded volume of the grains, imposing restrictions on their relative positions. For glass forming liquids, a simple frustrated lattice gas (FLG) has been introduced [5] that takes into account these steric effects and bridges complex fluids (glasses) and complex magnets (spin glasses). An infinite range version [6,7] has also been studied in the framework of replica theory, yielding a very rich phase diagram. In order to apply this model for granular systems, Nicodemi *et al* [8] introduced the effects of gravity in the model, studying a tilted $2d$ lattice while applying a sequence of taps, the particles following a diffusion-like Monte Carlo dynamics. Among several interesting properties, analogous to those found in real experiments, the system displays an inverse logarithmic compactation behavior, reversible-irreversible cycles, aging, as well as a localization transition, signalled by a zero diffusion constant, in which the particles get trapped into dynamical local cages. This transition point seems to correspond to the Reynolds (or dilatancy) transition observed in real systems. A lattice model has sev-

eral advantages. From the computational point of view, the simulation cost is much lower than molecular dynamics. From the theoretical side, besides the amenability to theoretical investigation explored here, it helps in grasping the fundamental concepts involved responsible for the complex observed phenomena.

In the same spirit as Sherrington and Kirkpatrick [9] introduced an exactly solvable version of the Edwards-Anderson model [10], here we introduce an infinite range version of the FLG considering L layers of N sites, connections being only between nearest neighbors layers (see fig.1). Each site may be occupied by a particle ($n_i = 0, 1$) having, for simplicity, only two possible spatial orientation, $S_i = \pm 1$. Although the grains can assume several spatial orientations (usually infinite), here we take the simplest case. The steric effects imposed by neighboring particles are felt as restrictions on the particle orientation, what is included in the hamiltonian as quenched, gaussian distributed lattice bonds J_{ij}^ℓ with $\overline{J_{ij}^\ell} = 0$ and $\overline{(J_{ij}^\ell)^2} = J/N$. Although the geometric frustration on the internal degrees of freedom should be considered as annealed at low densities and almost quenched at high ones, the quenched approximation is sufficiently good as can be seen from the $2d$ results [4,5]. Each layer has its own chemical potential satisfying $\mu_{\ell+1} > \mu_\ell$ (counting from top to bottom) that accounts for the effect of gravity and $\mu_\ell = g\ell/L$ in order to have a constant force. Thus, we consider the following Hamiltonian:

$$\mathcal{H} = - \sum_{i < j} \sum_{\ell=1}^{L-1} \left(J_{ij}^\ell S_i^\ell S_j^{\ell+1} + \frac{K}{N} \right) n_i^\ell n_j^{\ell+1} - \sum_{\ell=1}^{L-1} \mu_\ell \sum_i n_i^\ell \quad (1)$$

The parameter $K = -1 + K'$ may tune the repulsive/attractive (K' negative/positive) interaction between particles [7] and may be important to treat wet powders. Here, as in the original model, we consider $K = -J = -1$ ($K' = 0$). Notice that the value -1 appears originally in order to recover, in the limit $J \gg 1$, the Frustrated Percolation (FP) [4] constraint of only allowing non frustrated loops to be fully occupied. In this

limit, two given neighboring sites, only could be occupied ($n_i n_j = 1$) if the corresponding orientations satisfied the local disorder, $J_{ij} S_i S_j = 1$, otherwise at least one site should be empty ($n_i n_j = 0$). It is also important to point out that by changing the value of K , several new qualitatively different phases do appear, in both frustrated or not versions of the Blume-Emery-Griffiths (BEG) model (see [7] and references therein). In the limit where all sites are occupied, we get a layered version of the SK model (L-SK). This model has a continuous transition from a spin glass ($q_\ell \neq 0$) phase to a paramagnetic one ($q_\ell = 0, \forall \ell$) at $T_c^{SK} = 1/\sqrt{2x_c}$ where x_c is the lowest positive root of a polynomial recursively obtained by $P_L^{SK}(x) = P_{L-1}^{SK}(x) - x^2 P_{L-2}^{SK}(x)$ with $P_0^{SK} = P_1^{SK} = 1$. A similar result [12] has been found for a modified mean-field version of the McCoy-Wu model [13]. This critical temperature approaches unity as $L \rightarrow \infty$.

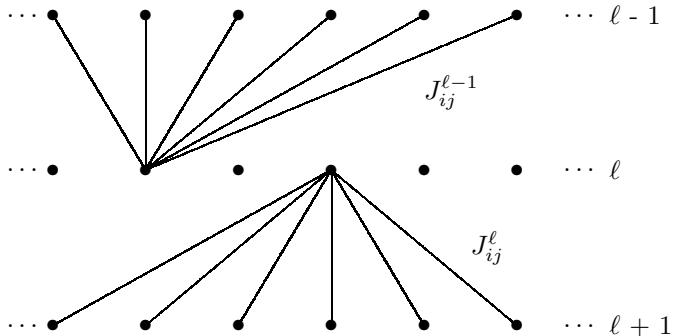


FIG. 1. System architecture with L layers, connections being only between nearest neighbors layers.

In evaluating the free energy, the trace is restricted to states with a given density ρ . Using standard techniques for dealing with disordered systems [14] and assuming replica symmetry, the free energy reads

$$f = \frac{\beta}{4} \sum_{\ell} q_{\ell} q_{\ell+1} - \frac{1}{2} \left(\frac{\beta}{2} - 1 \right) \sum_{\ell} d_{\ell} d_{\ell+1} + \beta \sum_{\ell} t_{\ell} d_{\ell} - \sum_{\ell} (\mu_0 + \mu_{\ell}) d_{\ell} - \frac{\beta}{2} \sum_{\ell} r_{\ell} q_{\ell} - \frac{L}{\beta} \ln 2 + \mu_0 \rho L - \frac{1}{\beta} \sum_{\ell} \int \mathcal{D}z \ln \{ 1 + \cosh(\beta \sqrt{r_{\ell}} z) e^{-\Xi_{\ell}} \} \quad (2)$$

where $\mathcal{D}z = dz/\sqrt{2\pi} \exp(-z^2/2)$ and the temperature $T = \beta^{-1}$ is a measure of the vibration imposed to the system. The order parameters are a diluted Edwards-Anderson $q_{ab}^{\ell} = \langle S^{a\ell} n^{a\ell} S^{b\ell} n^{b\ell} \rangle$ and the density $d_a^{\ell} = \langle n^{a\ell} \rangle$ while μ_0 accounts for the constraint $\rho = L^{-1} \sum_{\ell} d_{\ell}$ and

$$\Xi_{\ell} = \frac{\beta^2}{4} (q_{\ell+1} + q_{\ell-1}) - \frac{\beta}{2} \left(\frac{\beta}{2} - 1 \right) (d_{\ell+1} + d_{\ell-1})$$

$$-\beta(\mu_{\ell} + \mu_0) \quad (3)$$

The saddle point equations are $r_{\ell} = (q_{\ell-1} + q_{\ell+1})/2$ and

$$q_{\ell} = \int \mathcal{D}z \frac{\sinh^2(\beta \sqrt{r_{\ell}} z)}{[e^{\Xi_{\ell}} + \cosh(\beta \sqrt{r_{\ell}} z)]^2} \quad (4)$$

$$d_{\ell} = \int \mathcal{D}z \frac{\cosh(\beta \sqrt{r_{\ell}} z)}{e^{\Xi_{\ell}} + \cosh(\beta \sqrt{r_{\ell}} z)} \quad (5)$$

where $q_0 = d_0 = q_{L+1} = d_{L+1} = 0$. A global order parameter may be introduced as $Q = L^{-1} \sum_{\ell} q_{\ell}$.

There is a critical temperature T_c above which all q_{ℓ} are zero, that is, $Q = 0$. Figure 2 shows, for $L = 100$, the critical temperature as a function of density for several values of g . Notice that the bigger the density, the stronger should be the vibration in order to get a fluid state, similar to what happens for fixed density and increasing gravity. When $g = 0$ (no gravity), $d_{\ell} = \rho$ ($\forall \ell$) and $T_c = \rho T_c^{SK}$ where T_c^{SK} is the critical temperature of the L -layered SK model (see below). On the other limit, when $g \rightarrow \infty$ (strong gravity), in analogy with the layered SK model, the critical temperature is related with the smallest positive root x^* of a given polynomial, $T_c = 1/\sqrt{2x^*}$, depending on the density ρ . For $0 \leq \rho \leq 1/L$, we have $T_c = 0$ because all particles occupy the lowest layer and do not interact. For $1/L \leq \rho \leq 2/L$, some sites occupy the second lowest layer and the critical temperature is obtained with the root of $P_2(x)$. In general, for $(n-1)/L \leq \rho \leq n/L$, the relevant polynomial is $P_n(x)$. These polynomials are obtained recursively by

$$P_{\ell}(x) = \frac{P_{\ell-1}(x)}{\delta_{\ell L}(\rho L - L + 1)^2 + (1 - \delta_{\ell L})} - x^2 P_{\ell-2}(x) \quad (6)$$

with $P_0(x) = P_1(x) = 1$. In this limit, the critical temperature goes to unity for large L .

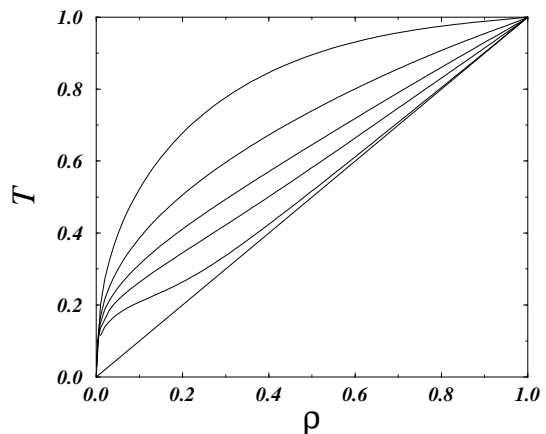


FIG. 2. Phase diagram T versus ρ for $L = 100$ and g from 0 (straight line) to 5 (top curve), showing the disordered phase ($q_{\ell} = 0, \forall \ell$) and a spin glass phase ($q_{\ell} \neq 0$).

The density and q profiles are shown in fig. 3 as a function of the system height ℓ/L . Interestingly enough, the density profile shows, even at low temperature, that frustration effects are important in preventing a close packed configuration, signaled by a density lower than one. It's important to stress that, in analogy with the FLG [6], there are two regimes of densities depending on the gravity: one is the L-SK regime for large g with the particles settling in the lowest possible layers disregard the geometric effects and the second and most interesting one, shown here, where the steric effects become important. Although the q -profile seems to vanish above a given height, it actually does not do so for finite L and as we approach the continuous limit ($L \rightarrow \infty$), a new transition settles down. From experiments and molecular dynamics simulation [16,17], as a function of the vibration, the system passes from a solid-like behavior to a fluid-solid coexistence region. After this onset of fluidization, the top layers become fluid-like, the particles having a great mobility. The interface between those regions decreases its height as the vibration increases. Although in this context a fluid regime means a situation where the particles present translational mobility, here we consider the case where the mobility is orientational, that is, a fluid layer will be one having $q_\ell = 0$. However, in some sense, both are a measure of the amount of geometrical constraints imposed on the particles by their neighbors. Moreover, when simulating the 3d system in absence of gravity [5], it can be seen that at the glass transition, the diffusion coefficient does vanish, corroborating our use of the term. For increasing values of L we can extrapolate the numerical results and find the critical layer, $\ell_c(T)$, separating the fluid region ($q_\ell = 0$) and the solid one ($q_\ell \neq 0$). The temperature where this first happens, signalling the onset of fluidization, is denoted by T_F and the transition is discontinuous from T_F up to T_{trc} , while continuous for $T_{trc} < T < T_c$. Notice that below T_F all non-empty layers have $q_\ell \neq 0$. The point T_{trc} is reminiscent of the tricritical point found in the disordered BEG model (remember that we have a varying chemical potential in the vertical axis). These information is summarized in figure 4. Notice that although in the figure 3 the top most layers have $q_\ell = 0$ below T_F , they are empty. Moreover, the density profile has been measured both in real experiments [15] as well as in simulations, showing that in the steady state, independently of the phase of the up and down motion of the heap, the density profile is always preserved. This fact, indicating that configurational properties may be obtained through appropriate averages, independently of the dynamics, supports our equilibrium results and has also led to thermodynamic theories of granular systems [18]. Also, as the granular temperature increases, there is an elevation of the center of mass of the system [11], given by $h_{CM} = (\rho L)^{-1} \sum_\ell \ell d_\ell$ and this is a function of both temperature and gravity.

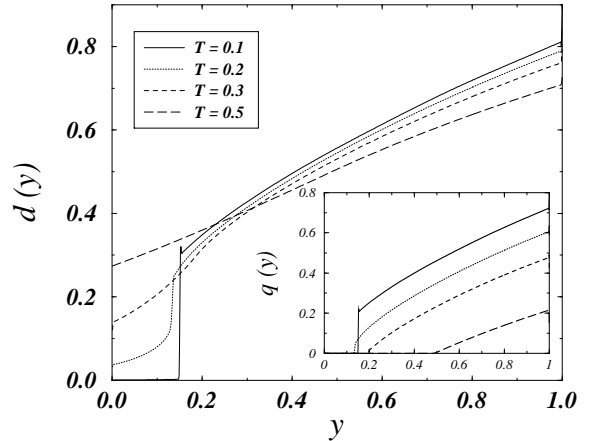


FIG. 3. Density profile as a function of $y = \ell/L$ for $L = 1000$, $\rho = 0.5$, $g = 1$ and several values of T . At high temperatures we recover the original mean field FLG as the density becomes uniform. Inset: profile of q_ℓ . Although the curve seems to go to zero above a certain layer, it actually does not do so for finite L . The onset of fluidization arrives at once for every layer.

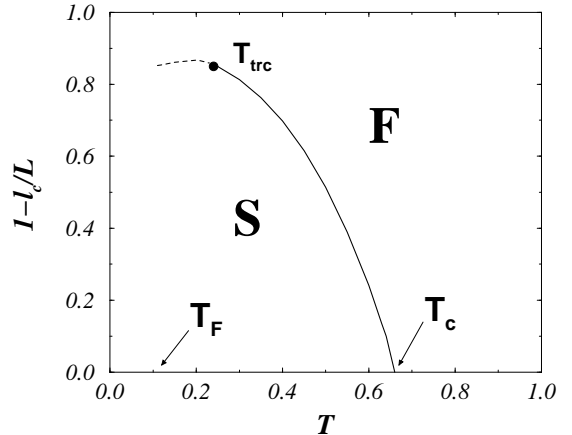


FIG. 4. Transition line $1 - \ell_c/L$ showing the higher, fluidized layers and the lower, solid ($q_\ell \neq 0$) ones for $g = 1$, $\rho = 0.5$ and large L . The onset of fluidization occurs at $T_F \simeq 0.11$ while the system is completely fluidized above $T_c \simeq 0.66$. For $T < T_F$ we have $q_\ell \neq 0$ for every non empty layer and since there is no longer a solid-fluid interface, just the material surface, we do not show the line. The transition is first order for $T_F < T < T_{trc} \simeq 0.24$ and continuous up to T_c .

In conclusion, we introduced an infinite range version of a frustrated lattice gas model [3,8] for granular systems and applied, to our knowledge for the first time, the replica formalism to these systems. In this mean field version, we are able to study stationary properties, obtaining the vibration, density and gravity dependent phase diagram as well as information on the density profile and the onset of fluidization.

There is a multitude of possibilities that still remain to be explored. First of all, the stability of the replica symmetric solution employed here and the behavior of the response functions, like the compressibility, for example. Also, the effects of segregation on polydisperse mixtures observed experimentally [1] and in the $2d$ model [21], can be included by allowing different degrees of frustration for each type of particle in the Hamiltonian [19]. Results on the $2d$ model show that the out of equilibrium dynamics, when the system is subject to small, continuous shaking [20], present aging in the two times correlation function $C(t, t_w)$ for the bulk density, remanent of the glassy nature of the model. In view of this, it would be extremely interesting to study in detail the mean-field equations for the dynamics [22]. Different coupling distributions, e.g. bimodal, may be studied by means of the TAP formalism [23], and in the limit of large L , the density and q profile should obey a set of coupled differential equations, from which some analytical results may be obtained. From the simulational point of view, research is in course to study how compactation and segregation are affected by interpolating from the $2d$ model to the mean field case, along with the effects of attraction ($K > -1$) between the particles, as in wet powders. Besides that, the fluidization transition may be detected on the simulation by measuring the mean squared displacement for each particle, $R_i^2(t)$ (instead of the system average) and comparing with its mean height.

Acknowledgments: I thank A. Coniglio, N. Lemke, M. Nicodemi, L. Peliti and M. Sellitto for very fruitful discussions, and the warm hospitality of the Dipartimento di Scienze Fisiche (Università di Napoli, Italy) during my stay. Work partially supported by the Brazilian agencies CNPq and FINEP.

- [1] H.M. Jaeger and S.R. Nagel 1992 *Science* **255** 1523; H.M. Jaeger, S.R. Nagel and R.P. Behringer 1996 *Rev. Mod. Phys.* **68** 1259
- [2] J.B. Knight, C.G. Fandrich, C.N. Lai, H.M. Jaeger and S.R. Nagel 1995 *Phys. Rev. E* **51** 3957
- [3] A. Coniglio and H.J. Herrmann 1996 *Physica A* **225** 1
- [4] A. Coniglio 1994 *Nuovo Cimento* **16D** 1027
- [5] M. Nicodemi and A. Coniglio 1997 *J. Phys. A* **30** L187
- [6] J.J. Arenzon, M. Nicodemi and M. Sellitto 1996 *J. Physique I* **6** 1143
- [7] M. Sellitto, M. Nicodemi and J.J. Arenzon 1997 *J. Physique I* **7** 945
- [8] M. Nicodemi, A. Coniglio and H.J. Herrmann 1997 *J. Phys. A* **30** L379; 1997 *Phys. Rev. E* **55** 3962
- [9] D. Sherrington and S. Kirkpatrick 1975 *Phys. Rev. Lett.* **35** 1792
- [10] S. Edwards and P.W. Anderson 1975 *J. Phys.* **F5** 965
- [11] S. Luding, H.J. Herrmann and A. Blumen 1994 *Phys. Rev. E* **50** 3100
- [12] B. Berche, P.E. Berche, F. Iglói and G. Palágyi 1998 *J. Phys. A* **31** 5193
- [13] B.M. McCoy and T.T. Wu, 1968 *Phys. Rev.* **176** 631; 1969 **188** 982
- [14] M. Mezard, G. Parisi and M.A. Virasoro 1987 *Spin Glass and Beyond* World Scientific.
- [15] E. Clement and J. Rajchenbach 1991 *Europhys. Lett.* **16** 133
- [16] J. Gallas, H.J. Herrmann and S. Sokolowski 1992 *Physica A* **189** 437
- [17] Y.-H. Taguchi 1993 *Europhys. Lett.* **24** 203
- [18] H. Hayakawa and D.C. Hong 1997 *Phys. Rev. Lett.* **78** 2764
- [19] J.J. Arenzon and M. Nicodemi, in preparation
- [20] M. Nicodemi and A. Coniglio, cond-mat/9803148
- [21] E. Caglioti, A. Coniglio, H.J. Herrmann, V. Loreto and M. Nicodemi 1998 *Europhys. Lett.* in press
- [22] L.F. Cugliandolo and J. Kurchan 1993 *Phys. Rev. Lett.* **71** 173; 1994 *J. Phys. A* **27** 5749
- [23] D.J. Thouless, P.W. Anderson and R.G. Palmer 1977 *Phyl. mag.* **35** 593